# We are IntechOpen, the world's leading publisher of Open Access books Built by scientists, for scientists

6,900
Open access books available

186,000
International authors and editors

200M
Downloads

Our authors are among the

154
Countries delivered to

TOP 1%
most cited scientists

12.2%
Contributors from top 500 universities


WEB OF SCIENCE™

Selection of our books indexed in the Book Citation Index in Web of Science™ Core Collection (BKCI)

## Interested in publishing with us?
## Contact book.department@intechopen.com

Numbers displayed above are based on latest data collected.
For more information visit www.intechopen.com

# 4

# Fast Charged Particles and Super-Strong Magnetic Fields Generated by Intense Laser Target Interaction

Vadim Belyaev and Anatoly Matafonov
*Central Research Institute of Machine Building*
*Russian Federation*

## 1. Introduction

The development of a new generation of solid-state lasers has resulted in unique conditions for irradiating laser targets by light pulses, with radiation intensity ranging from $10^{17}$ to $10^{21}$ W/cm$^2$ and a duration of 20 - 1000 fs.

At such intensities, the laser pulse produces superstrong electric fields which could not be obtained earlier and considerably exceed the atomic electric field of strength $E_a$ = 5.14×10$^9$ V/cm. In these conditions, there arises a new physical picture of laser pulse interaction with plasma produced when the pulse leading edge or a pre-pulse affects solid targets. Laser radiation is rather efficiently transformed into fluxes of fast charged particles such as electrons and atomic ions. The latter interact with the ambient material of the target, which leads to the generation of hard X-rays, when inner atomic shells are ionized, and to various nuclear and photonuclear reactions.

One important area in investigating the interaction of sub-picosecond laser pulses with solid targets is related to the important role which arising superstrong quasistatic magnetic fields and electronic structures play in laser plasma dynamics. This area of research became most attractive after carrying out the direct measurements of quasistatic magnetic fields on the Vulcan laser system (Great Britain) (Tatarakis et al., 2002), in particular, after the pinch effect has been found experimentally in laser plasma (Beg et al., 2004).

The relativistic character of laser radiation with intensity $I$ is realized at the magnitude of a dimensionless parameter $a > 1$. This parameter represents the dimensionless momentum of the electron oscillating in the electric field of linearly polarized laser radiation and can be expressed as

$$a = \frac{eE}{mc\omega} = 0.85\left(\frac{\lambda}{\mu\mathrm{m}}\right)\left(\frac{I}{10^{18}\,\mathrm{W/cm^2}}\right)^{\frac{1}{2}} \tag{1}$$

$$\frac{E}{\mathrm{V/cm}} = 27.7\left(\frac{I}{\mathrm{W/cm^2}}\right)^{\frac{1}{2}} \tag{2}$$

where $e$ and $m$ are the charge and mass of the electron, respectively, $E$ is the amplitude of electric field strength (in units of V/cm) of laser radiation, $\lambda$ is the radiation wavelength (in μm), $\omega$ is the frequency of laser radiation, $c$ is the speed of light, and $I$ is the radiation intensity (in W/cm$^2$).

Terawatt-power laser systems of moderate size can fulfill the condition $a > 1$, which corresponds to the electric field strength above $10^{10}$ V/cm. In such intense fields, the overbarrier ionization of atoms occurs in atomic time on the order of $10^{-17}$ s, and the electrons produced are accelerated and reach MeV-range relativistic energies during the laser pulse.

The acceleration of atomic ions in femto- and picoseconds laser plasmas constitutes a secondary process. It is caused by the strong quasistatic electric fields arising due to spatial charge separation. Such separation is related to the motion of a bunch of fast electrons. For laser radiation intensities exceeding $I \geq 10^{18}$ W/cm$^2$, it is possible to obtain directed beams of high-energy ions with the energies $\varepsilon_i > 1$ MeV.

The generation of high-energy proton and ion beams in laser plasma under the action of ultrashort pulses is a quickly developing field of investigations. This is explained, in particular, by their important applications in such fields as proton accelerators, the study of material structure, proton radiography, the production of short-living radioisotopes for medical purposes, and laser controlled fusion (Umstadter, 2003; Mourou et al., 2006). For a laser radiation intensity of $I \geq 10^{18}$ W/cm$^2$, a number of nuclear reactions can be initiated that have only been realized in elementary particle accelerators (Andreev et al., 2001).

Later on, we will consider the principal mechanisms for generating fast charged particles and quasistatic magnetic fields in laser plasmas, as well as experimental results obtained both abroad and on the native laser setup NEODIM in the Central Research Institute of Machine Building (Russ. abbr. TsNIIMash) (Korolev, Moscow reg.) (Belyaev et al., 2004; Belyaev et al., 2005).

## 2. Generation of fast electrons in laser plasma

In irradiating a target by a high-intensity ultrashort laser pulse, the radiation energy is rather efficiently converted into the energy of fast electrons which later partially transfer their energy to the atomic ions of the target. Presently, several mechanisms are being discussed concerning the generation of fast electrons when a laser pulse affects plasma with a density well above the critical value. If the laser pulse is not accompanied by a pre-pulse (the case of high contrast), then the laser radiation interacts with plasma of a solid-state density, possessing a sharp boundary. In this case, the mechanism of `vacuum heating' is realized (Brunel, 1987), as is the so-called $\mathbf{v}\times\mathbf{B}$ mechanism (Wilks et al., 1992) (here, $\mathbf{B}$ is the magnetic field induction of the laser field) caused by a longitudinal ponderomotive force acting along the propagation direction of the laser pulse). This $\mathbf{v}\times\mathbf{B}$ mechanism becomes substantial at relativistic intensities where the energy of electron oscillations is comparable with or exceeds the electron rest energy $mc^2$ = 511 keV - that is, for the parameter $a > 1$ [see formula (1)]. In addition, fast electrons can be generated on the critical surface of plasma at a plasma resonance ( Gus'kov et al., 2001; Demchenko et al., 2001) if the vector of the laser radiation electric field has a projection along the density gradient (usually at an inclined incidence of laser radiation to target) and the laser frequency coincides with the plasma

frequency. In contrast to the ponderomotive **v**×**B** mechanism, vacuum heating and resonance absorption arise at nonrelativistic (substantially lower, with $a < 1$) intensities as well. In the case of the ponderomotive mechanism, the average energy of fast electrons can be estimated as the maximum energy of transverse electron oscillations in an electromagnetic field, which in the general case takes a relativistic value. In a underdense part of the laser plasma, we have

$$\varepsilon_e = mc^2\left[\left(1+\frac{Q}{Q_0}\right)^{\frac{1}{2}}-1\right],\ Q = I\lambda^2,\ Q_0 = 1.37\times 10^{18}\,\frac{\mathrm{W}}{\mathrm{cm}^2}\,\mu\mathrm{m}^2 \tag{3}$$

In the ultrarelativistic limit $Q \rangle\rangle Q_0$, we hence obtain

$$\varepsilon_e = mc^2\left(\frac{Q}{Q_0}\right)^{\frac{1}{2}}.$$

By contrast, in the nonrelativistic limit $Q \langle\langle Q_0$, we derive from formula (3) that

$$\varepsilon_e = mc^2\frac{Q}{2Q_0}.$$

In the overdense part of the plasma, the ponderomotive heating of electrons is noticeably weaker due to a difficult penetration of the laser field into this region.
In the case of vacuum heating, the maximum energy of an electron flying into the depths of a dense target is given by the formula similar to equation (3), however, with a different numerical factor.
There is one more mechanism for generating fast electrons in the underdense part of plasma in front of a target due to the betatron resonance in the arising magnetic field (Pukhov, 2003). In this regime, electrons are accelerated by the transverse ultrarelativistic electric field of the laser wave in the direction of wave polarization, and the azimuthal magnetic field produced by the current of fast electrons is responsible for the magnetic part of the Lorentz force. This force turns electrons in such a way that they gradually change to the opposite direction of motion. In the case of an exact betatron resonance, the reflection occurs at the instant when the transverse electric field changes its direction, so the electrons are accelerated at all times. This mechanism yields an energy of fast electrons three times greater than formula (3) does:

$$\varepsilon_e = 3mc^2\left(\frac{Q}{Q_0}\right)^{\frac{1}{2}}. \tag{4}$$

There are also further mechanisms of electron acceleration that require special experimental conditions, for example, the wake field acceleration (Esarey, 1996; Amiranoff, 1998). In the case of resonance absorption, the electric field near the plasma critical surface is much stronger than that of incident laser radiation. The result is that the heating of electrons upon their impact with atomic ions is greater than follows from formulae (3) and (4).

Electrons are also accelerated by a transverse ponderomotive force (acting in the radial direction) due to a focal distribution of laser intensity. This acceleration leads to the maximum electron energy also expressed by formula (3) (in the underdense part of plasma) if electrons succeed in acquiring this energy moving from the focus to the periphery during the laser pulse. Thus, the duration $\tau$ of a laser pulse should meet the inequality $\tau \rangle\rangle m\omega R/eE$ (in the nonrelativistic case). Here, $R$ is the radius of the focal spot of a laser beam. This inequality holds for picosecond- and longer-duration laser light pulses with an intensity on the order of $10^{16}$ W/cm$^2$. In fields with an intensity of $10^{18}$ W/cm$^2$, the right-hand side of this inequality reaches dozens of femtoseconds, whereas in the overdense part of plasma this ponderomotive force is noticeably weaker.

We have discussed the above mentioned mechanisms in more detail in our article (Belyaev et al., 2008).

We suggested and investigated the new mechanism of high-energy electrons formation in ultra-high intensity laser pulse interaction with solid targets (Belyaev, 2004). This investigation is an attempt to reveal and describe, based on the model suggested, the high-energy electron formation mechanism in laser plasmas so as to derive theoretical dependences which would represent specific relations between the parameters of fast electrons, laser radiation and target substance.

Any theory can be accepted only after reliable experimental verification. The degree of reliability is determined not only by the sufficient diversity of independent experimental data, but also by the ability to choose out of these data those best representative of the overall pattern. Analysis of numerous experiments to measure energy of fast electrons formed in laser plasmas shows that with a particular laser facility, given its available radiation intensity, fast electron maximum energy can be determined most closely. Generally, it is electron maximum energy values that are most widely presented in experimental investigations. This is motivated not only by experimenters' striving to get extreme record-breaking output parameters, but also by the possibility to most closely determine the electron maximum energy around their spectrum extrapolation at specified intensity of laser radiation incident on a target. On this basis we will establish our theoretical model of the maximum-energy electron formation process for a given laser radiation intensity.

Without going into details of magnetic field generation mechanisms, it can be noted that a vortical electron structure develops eventually in plasma. Given the applied electric field (constituent of the incident laser radiation) and the dominance of tunnel ionization, a great number of electrons (practically determined by solid density) are accelerated. This current of electrons generates a magnetic field which bends their trajectory. Under certain conditions these trajectories can close at skin-layer depth within larmor-radius circle. The high electron density and, correspondingly, the circular current strength cause super-strong magnetic fields generation.

Condition for such fields generation can be written as a condition for electron movement around such a circle in the form of a balance between the centrifugal force and the Lorentz force:

$$\frac{mV^2}{r} = \frac{eVB}{c}, \tag{5}$$

where $r = \delta/2$, $\delta$ - skin-layer thickness, $e$, $m$, $V$ – charge, mass, electron velocity, $c$ – velocity of light, $B$ – magnetic induction in the electron orbit.
Taking electromagnetic field penetration depth $\delta$ to be equal to incident radiation wave length $\lambda$, we have $r = \lambda / 2$.
Given the relationship between mass and velocity, the kinetic energy change due to the action of the forces applied is always equal to

$$E_{KIN} = (m_V - m_0)c^2 = m_0c^2(\gamma - 1), \tag{6}$$

where $m_V$ - relativistic mass, $m_0$ – electron rest mass, $\gamma = 1/\sqrt{1 - V^2/c^2}$ - relativistic factor.
Considering:

- relativistic expression of electron momentum

$$\mathbf{P} = \mathbf{p} - \frac{e}{c}\mathbf{A} \tag{7}$$

where $V$ – electron velocity;

- use of generalized momentum

$$\mathbf{P} = \mathbf{p} - \frac{e}{c}\mathbf{A}, \tag{8}$$

where **p** – ordinary momentum (8), **A** – vector-potential;

- magnetic field $B$ cylindrical symmetry: $B_X = 0$; $B_Y = 0$; $B_Z = -\frac{\partial A_X}{\partial y} = B$, which allows to put $A = Br$ and

$$P = m_0V = \frac{e}{c}Br \tag{9}$$

So from (6) – (9) we have

$$E_{KIN} = m_0c^2\left[1 + \left(\frac{eBr}{m_0c^2}\right)^2\right]^{\frac{1}{2}} - m_0c^2, \tag{10}$$

To find the electron maximum kinetic energy at specified intensity of laser radiation incident on the target we need the maximum value of $B$ – magnetic field induced in laser plasma. This value can be estimated using the energy conservation law.
Omitting calculations we can use the following formula easy to keep in mind:

$$B_{MAX}\ [\mathrm{Gs}] = 10^{-1}\sqrt{J[\mathrm{W/cm^2}]}, \tag{11}$$

Substitution this formulae in expression (10) for kinetic electron energy gives:

$$E_{KIN} = 0{,}5\left[1 + \frac{9J\lambda^2}{10^{18}}\right]^{\frac{1}{2}} - 0{,}5, \tag{12}$$

where intensity $J$ expressed in W/cm², $\lambda$ – in micrometer, kinetic energy – MeV.
Graph of this dependence show Fig. 1 by curve 1.

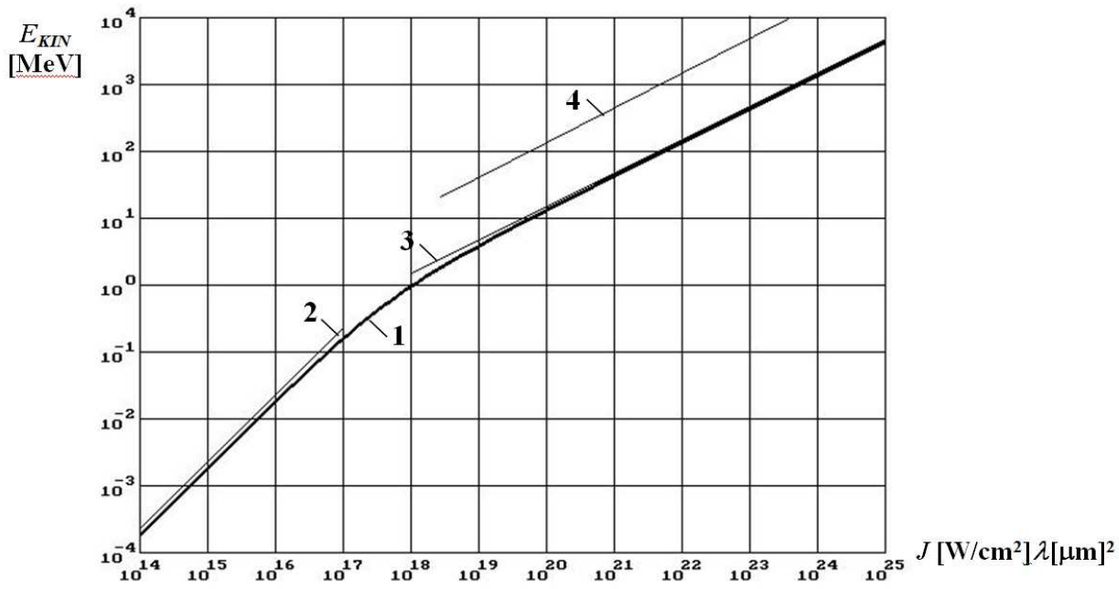


Fig. 1. Dependence of electron kinetic energy on laser radiation intensity.

Consider limiting cases.

1. $E_{KIN} = m_0c^2 = 0{,}5$ MeV.

Expression (12) gives this value at intensity

$$J_R = \frac{1}{3}10^{18}\left[\frac{1}{\lambda\ [\mu\text{m}]}\right]\frac{\text{W}}{\text{cm}^2}, \tag{13}$$

The intensity $J_R$ can be called as relativistic intensity.

2. $E_{KIN} \langle\langle m_0c^2$; $J < J_R$.

In this case

$$E_{KIN} = 2{,}25\frac{J\lambda^2}{10^{18}}, \tag{14}$$

Graph of this dependence show at Fig. 1 by curve 2.

3. $E_{KIN} \rangle\rangle m_0c^2$; $J > J_R$.

For this case

$$E_{KIN} = 1{,}5\left(\frac{J\lambda^2}{10^{18}}\right)^{\frac{1}{2}}, \tag{15}$$

and graph of this dependence show on Fig. 1 by curve 3.
Equations obtained for small ($< m_0c^2$) and large ($> m_0c^2$) values of kinetic energy agree with those in use for calculations of particle energy in a cyclotron and in a betatron,

correspondingly. In both cases electrons are accelerated under the action of an electric field. In a cyclotron, this is a periodically changing electric field applied externally. In a betatron, this is a vortex electric field occurring with axisymmetric magnetic field rise in time. In laser plasmas a magnetic field is generated giving rise to a vortex electric field accelerating electrons. Thus the laser-plasma electron acceleration mechanism resembles the betatron case.

Equation (10) for electron kinetic energy was derived on the assumption that the electron acceleration is governed only by the laser radiation incident on the target without considering the processes going within the target substance, specifically, ionization process. Formally, it is reflected in the fact that the skin-layer size is determined by the laser radiation frequency

$$\delta = c/\nu = 2\pi c/\omega = \lambda \,, \tag{16}$$

meaning that the laser radiation frequency $\omega$ is an effective frequency. This assumption is true only at the first stage of interaction with the substance when a vortical electron structure develops on skin-layer scales, its characteristic size being in accordance with (16). This structure is unstable and there is a possibility of its transformation to smaller-scale structures. This process is known as a dynamic pinch.

It is demonstrated in (Belyaev & Mikhailov, 2001) that in case of laser plasmas produced by the action of high-intensity ($J > 10^{16}$ W/cm$^2$) laser radiation of ultrashort duration ($\tau < 10^{-12}$ sec) on a solid target this process is of quantum nature and can be described by the diffusion equation. Without going into the process nature, note that under tunnel ionization the vortical electron structure generated on skin-layer scales (16) transforms to another one, its characteristic size now being determined by the ionization frequency as an effective frequency at the next stage of laser radiation interaction with the substance, i.e. at the stage of tunnel ionization development:

$$l_i = 2\pi c/\omega_i \,, \tag{17}$$

Assuming that the vortical electron structure transformation process goes with the magnetic flow kept unchanged, we have

$$B_0\lambda^2 = B_i l_i^2 \,, \tag{18}$$

where $B_i$ – magnetic field within the vortical structure, its characteristic size $l_i$, being determined by (17). Such a vortical structure provides the following kinetic energy to the electrons:

$$E_{кин} = eB_i l_i = eB_0 \frac{\lambda^2}{l_i} \,, \tag{19}$$

Equation (19) determines the maximum energy of the small group (tail) of high-energy electrons. This dependence can be represented via the energy or ionization potential of the target substance atoms:

$$E_{KIN} = eB_0\lambda\frac{\omega_i}{\omega} = 1.5\left(\frac{J\lambda^2}{10^{18}}\right)^{\frac{1}{2}}\frac{\omega_i}{\omega} = 1{,}5\left(\frac{J\lambda^2}{10^{18}}\right)^{\frac{1}{2}}\frac{I}{\hbar\omega} \quad \text{[MeV]}, \tag{20}$$

Here $J$ is in W/cm$^2$, $\lambda$ - in μm, $I$ and $\hbar\omega$ - in eV. This dependence is plotted in Fig. 1 (curve 4).

The equation obtained demonstrates the proportionality between the electron energy and ionization frequency, hich determines physical nature of the electron acceleration process. The physics of the electron acceleration processes as a result of high-intensity laser radiation action on a substance is closely related to the physics of the ionization processes in superatomic intensity fields.

The ionization frequency is generally one or two orders higher than the laser one. This results in the high acceleration rate and electron energy.

The process of dynamic pinch development give rises formation of high-energy tail (20) and has threshold nature. Our estimations give value of threshold $0.31\times10^{18}$ – $3.2\times10^{19}$ W/cm$^2$. Threshold smearing evidences for stochastic character of the process.

The good agreement between theory and experiment (Matafonov & Belyaev, 2001; Malka & Miquel, 1996; Borodin et al., 2000; Nickles et al., 1999; Ledingham & Norreys, 1999; Cowan et al., 1999; He et al., 2004; Mangles et al., 2005) suggests the realizability of the proposed high-energy electron formation mechanism in laser plasmas.

In our article (Belyaev, Kostenko et al., 2003) we also have investigated cyclotron mechanism of electron acceleration.

The magnetic activity of picosecond laser plasma offers new mechanisms for the generation of fast electrons due to the presence of such strong quasistatic magnetic fields regardless of the mechanisms of their origin. Such a possibility is related to the emergence of cyclotron resonances when the laser frequency $\omega$ coincides with the Larmor gyration frequency $\Omega = eB_0/m_rc$ of an electron in an external constant magnetic field with the induction $B_0$ (here, $e$ and $m_r$ are the charge and relativistic mass of the electron, respectively; $c$ is the speed of
light). Indeed, the typical laser frequency $\omega$ (in the Hartree atomic system of units) is on the order of 0.05 a.u. and coincides with the cyclotron frequency at an induction of $B_0 = 7$ a.u. ~ 100 MG. This value may become much greater with allowance made for the relativistic increase in electron mass, which is typical at laser radiation intensities on the order of $10^{19}$ - $10^{20}$ W/cm$^2$.Hence, the generation of a constant magnetic field results in stronger interaction of laser radiation with plasma. The situation is to a certain extent similar to the radiation self-focusing effect, in which case the variations in the refraction index of the medium in the field of a laser wave influence wave propagation through the medium.

In the general relativistic case, the interaction of electrons with the field of a laser wave and with the constant magnetic field $\mathbf{B}_0$ is written out in the form

$$\frac{\mathrm{d}\mathbf{p}}{\mathrm{dt}} = e\left\{\mathbf{E} + \frac{1}{c}\mathbf{v}\times\left(\mathbf{B}+\mathbf{B}_0\right)\right\} \tag{21}$$

for electrons possessing a momentum $\mathbf{p}$ and a velocity $\mathbf{v}$.

For circular polarization, the problem is solved analytically, whereas in the general case of linear polarization the problem reduces to a system of nonlinear equations, which can only be solved numerically. The solution to these equations is specific in that there are resonances between the periodicmotion of electrons in the magnetic field and electron oscillations in the field of the laser wave. This fact leads to drastic changes in electron trajectory and energy at certain instants of time.

Figure 2 depicts the variations in the kinetic energy of an electron (a) and its trajectory (b) for motion with the zero initial velocity in a field with a radiation intensity of $10^{20}$ W/cm$^2$ and a frequency that is at resonance with the cyclotron frequency (Belyaev & Kostenko, 2003). The constant magnetic field is normal to the polarization of laser radiation. One can see that an electron acquires an energy of approximately 100MeV in a time on the order of hundreds of femtoseconds.

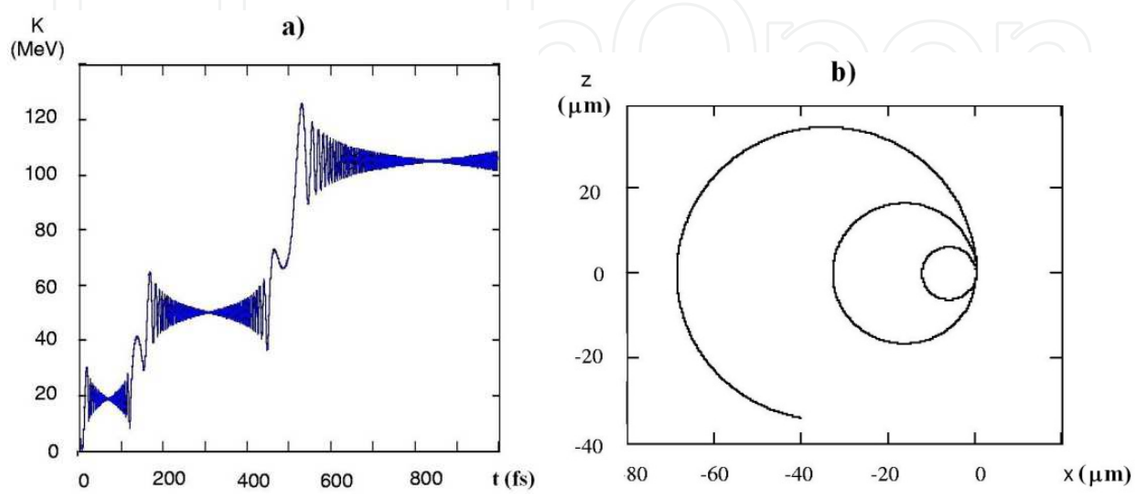


Fig. 2. Electron kinetic energy (a) and trajectory (b) in a linearly polarized laser wave with an intensity of $10^{20}$ W/cm$^2$ and a constant transverse magnetic field in the resonance case of $\Omega = \omega$.

Electron acceleration in the field of a circularly polarized laser wave propagating along a strong magnetic field was theoretically investigated in lectures (Pavlenko, 2002). It was shown that the relativistic factor of the electron may increase by an order of magnitude under a high intensity of laser radiation.

## 3. Generation of fast protons and ions in the interaction of ultrashort high-intensity laser pulses with solid targets

On the basis of the results of experimental and theoretical investigations performed in recent years, one can determine the following ranges for product plasma parameters: the electron temperature is about 1 to 10 keV; the mean energy of "fast" electrons is about 0.1 to 10 MeV (the maximum energy is as high as 300 MeV); the mean energy of fast ions ranges from several hundred keV units to a few MeV units (the maximum energy is 430 MeV); the relativistic longitudinal ponderomotive pressure of laser light is 1 to 50 Gbar; and the amplitudes of the electric field and spontaneous-magnetic-field strength range, respectively, between about $10^9$ and $10^{12}$ V/cm and between about 1 and 500 MG (Belyaev et al., 2008; Salamin et al., 2006). Product terawatt-pulse picosecond laser plasmas appear to be some kind of a "table" pulsed "microaccelerator" and a nuclear "microreactor," which is relatively compact and cheap and on which one must not impose special radiation-safety requirements. Such a source admits a relatively simple possibility for controlling energy and other parameters of corpuscular and electromagnetic radiations.

At the present time, the production of high-energy proton beams in laser plasmas under the effect of ultrashort pulses is a rapidly developing field of investigations (Carrier et al., 2009; Fucuda et al., 2009; Yan et al., 2009; Willingale et al., 2009; Gonoskov et al., 2009; Psikal et al., 2010; Huang et al., 2010).

Several models that claim for explaining observed results that concern the production of directed beams of high-energy protons were proposed in theoretical investigations. One of them is based on the mechanism of proton acceleration at the front surface of the target owing to the ponderomotive pressure of a laser pulse (Sentoku et al., 2003; Maksimchuk et al., 2000). According to a different model (MacKinnon et al., 2001; Wilks et al., 2001), relativistic hot electrons produced by a laser field in a solid-state target penetrate through the target, and some electrons escape from the rear surface of the target to a distance of about the Debye radius. These electrons generate an electrostatic field at the rear surface of the target. This field, which may exceed $10^{12}$ V/cm, accelerates protons.

However, the efficiency of the proposed proton acceleration mechanisms has so far been debated (Salamin et al., 2006). In view of this, the our experimental studies were aimed at exploring various mechanisms of the acceleration of fast protons in laser plasmas under identical conditions of the irradiation of a solid-state target at a laser-radiation intensity of about $2\times10^{18}$ W/cm$^2$.

The experiments in question were performed at the 10-TW picosecond laser facility Neodymium (Belyaev, Vinogradov et al., 2006). This laser facility has the following laser-pulse parameters: a pulse energy of up to 10 J, the wavelength of 1.055 μm, and the pulse duration of 1.5 ps. Its focusing system, which is based on an off-axis parabolic mirror whose focal length is 20 cm, ensures a concentration of not less than 40% of the laser beam energy within a spot $D$ = 15 μm in diameter and, accordingly, an average intensity of $10^{18}$ W/cm$^2$ at the target surface and a peak intensity of $2\times10^{18}$ W/cm$^2$.

Laser radiation generated by the Neodymium facility is characterized by the presence of two prepulses—one of picosecond and the other of nanosecond duration. The first prepulse appears 14 ns before the main laser pulse; it has a duration of 1.5 ps and an intensity below $10^{-8}$ with respect to the main pulse. The second prepulse results from amplified spontaneous emission. Its FWHM duration is 4 ns, while its intensity with respect to the main pulse is below $10^{-8}$.

The layout of the experiment is shown in Fig. 1. A beam of linearly polarized laser radiation of *p*-type polarization is focused by an off-axis parabolic mirror onto the surface of a solid-state target (T) at an angle of 40° with respect to the normal to the target surface. For targets, we employed slabs from LiF and Cu 1 to 30 mm in thickness and the Al, Cu, and Ti foils 1 to 100 μm in thickness. The targets were arranged in a vacuum chamber 30 cm in diameter and 50 cm in height. The pressure of the residual gas in the chamber was not more than $10^{-3}$ torr.

Detectors D1 based on CR-39 track detectors of size 24 to 20 mm and equipped with aluminum filters of different thickness, from 11 to 100 μm, which make it possible to cut off the energy interval 0.8–3.5 MeV for protons, were used to detect protons and to measure their energy spectrum. The detectors D1 were arranged upstream and downstream of the target at a distance of 20 mm from it along the normal.

The secondary activated targets D2, which were manufactured from LiF, Cu, and Ti and which are characterized by different threshold energies for (*p, n*) reactions (from 1.88 MeV for $^7$Li to 5 MeV for $^{48}$Ti), were also used to detect protons and to determine their number and maximum energy. The secondary activated targets D2 were slabs $30\times30$ mm$^2$ in cross-

sectional dimensions and 1 to 6 mm in thickness and were installed at the same positions as the track detectors D1. Thus, either the track detectors D1 or the secondary activated targets D2 were used in our experiment.

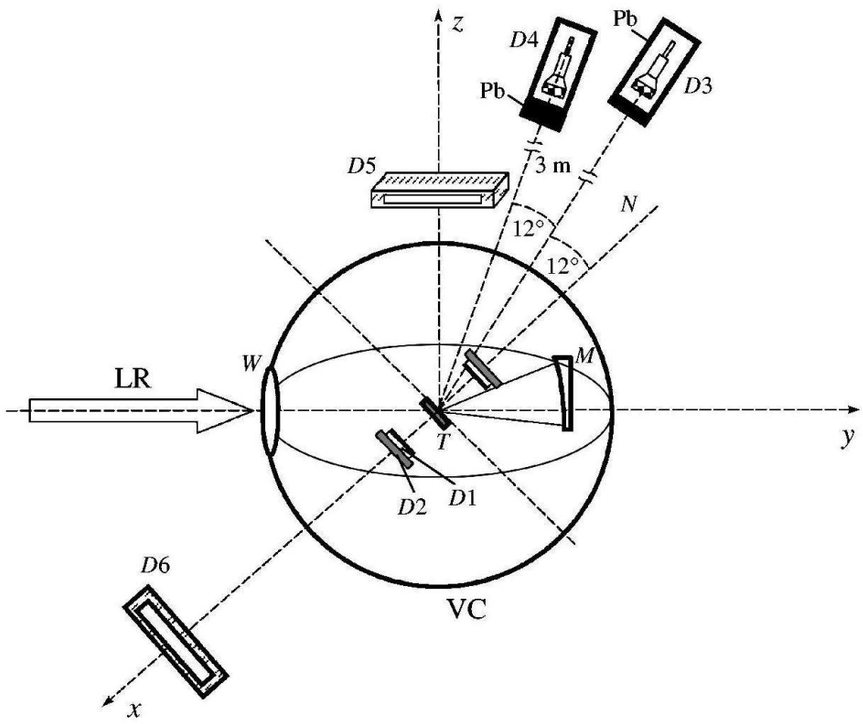


Fig. 3. Layout of the experiment: (T) target, (VC) vacuum chamber, (W) vacuum-chamber window; (M) off-axis parabolic mirror, (LR) laser radiation, (*N*) normal to the target, (D1) CR-39 track detectors equipped with aluminum filters, (D2) secondary activated targets from LiF, Cu, and Ti, (D3, D4) scintillation detectors for gamma radiation, and (D5, D6) neutron detectors on the basis of helium counters. Detectors D1–D4 and D6 lie in the *xy* plane.

Two scintillation detectors D3 and D4 positioned at distances of 4.3 and 3.0 m from the target, respectively, were used to record hard x-ray radiation. Lead filters 8 cm thick for D3 and 13.5 cm thick for D4 were installed in front of the detectors. The detectors D3 and D4 are scintillation detectors on the basis of plastic scintillators ∅5×10 cm in dimension. The detectors D3 and D4 were used to record hard x-ray photons of energy 0.5 to 10 MeV.

The detectors D5 and D6, which are based on helium counters, were used to determine the yield of neutrons generated in (*p, n*) reactions. The detector D5 was arranged along the tangent to the target surface at a distance of 25 cm, while the D6 detector was positioned behind the target at a distance of 60 cm. The detectors D5 and D6 consisted of the following units: a block of neutron counters on the basis of three CNM-18 helium counters, a voltage transducer, a signal-selection device, and a power amplifier. The side surfaces of the detectors D5 and D6 were surrounded by polyethylene 2 cm thick.

The layout of the experimental facility used to study various mechanisms of fast-proton production is displayed in Fig. 4. As targets, we employed metallic foils from titanium 30

$\mu$m thick (see Figs. 4*a* and 4*b*) and a LiF plate 6 mm thick (see Fig. 4*c*). As the secondary, activated, target, we took a LiF plate 6 mm thick. In the case presented in Fig. 4*c*, the primary target serves as the activated target as well.

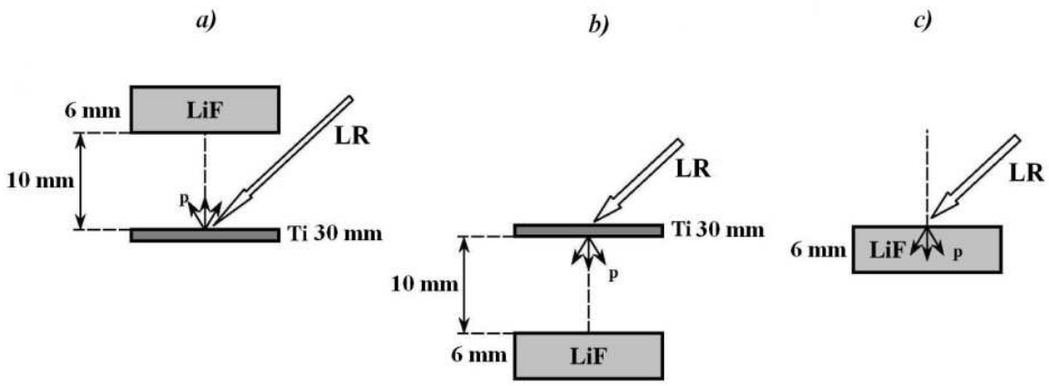


Fig. 4. Layout of experiments aimed at studying various mechanisms of the acceleration of fast protons: (*a*) acceleration of protons from the front surface of the target toward the laser pulse, (*b*) acceleration of protons from the rear surface of the target in the outward direction, and (*c*) acceleration of protons from the front surface of the target in the inward direction.

Taking into account the solid angle covered by the detector D5 and its efficiency, we found that the number of neutrons generated on average in the LiF secondary, activated, target over 4π sr per laser pulse is 50 in the first case (see Fig. 4*a*), about $2\times10^3$ in the second case (see Fig. 4*b*), and about $2\times10^2$ in the third case (see Fig. 4*c*).

The number of fast protons can be estimated by the formula $N_p \cong Y_n/(n\sigma l_i)$, where $Y_n$ is the yield of neutrons from the reaction $^7$Li($p$, $n$)$^7$Be, $n$ is the concentration of $^7$Li atoms in the target, $\sigma \approx 60$ mb (Youssef et al., 2006) is the cross section for the reaction $^7$Li($p$, $n$)$^7$Be at proton energies around 1.9MeV, and $l_i$ is the proton braking length in the target. At distances longer than $l_i$, protons have have energies below the threshold energy of 1.88 MeV, so that the reaction $^7$Li($p$, $n$)$^7$Be, which leads to neutron production, cannot proceed. Under the conditions of our experiments, $l_i \approx 10$ μm. Taking into account the yield of neutrons for the three cases considered here, we ultimately find that the number of accelerated protons from the front surface toward the laser pulse that have an energy in excess of 1.88 MeV is $10^7$; the number of protons accelerated from the rear surface of the target in the outward direction is $4\times10^8$, while the number of protons accelerated from the front surface in the inward direction is $4\times10^7$. Thus, the results of our experiments have revealed that the proton-acceleration process occurs most efficiently in the case of proton acceleration from the rear surface of the target in the outward direction.

This conclusion is also confirmed by the results obtained by measuring the spectra of fast protons for various mechanisms of their acceleration.

Figures 5 shows the measured spectra of protons for various proton-acceleration mechanisms. These spectra were obtained both by using track detectors CR-39 equipped with aluminum filters of various thickness and by using the activation procedure. From these spectra, it follows that the energy distribution of fast protons corresponds to the Boltzmann distribution at a temperature of 180 keV for protons accelerated from the front surface of the target toward the laser pulse, a temperature of 500 keV for protons accelerated

from the rare surface in the outward direction, and a temperature of 250 keV for protons accelerated from the front surface of the target in the inward direction.

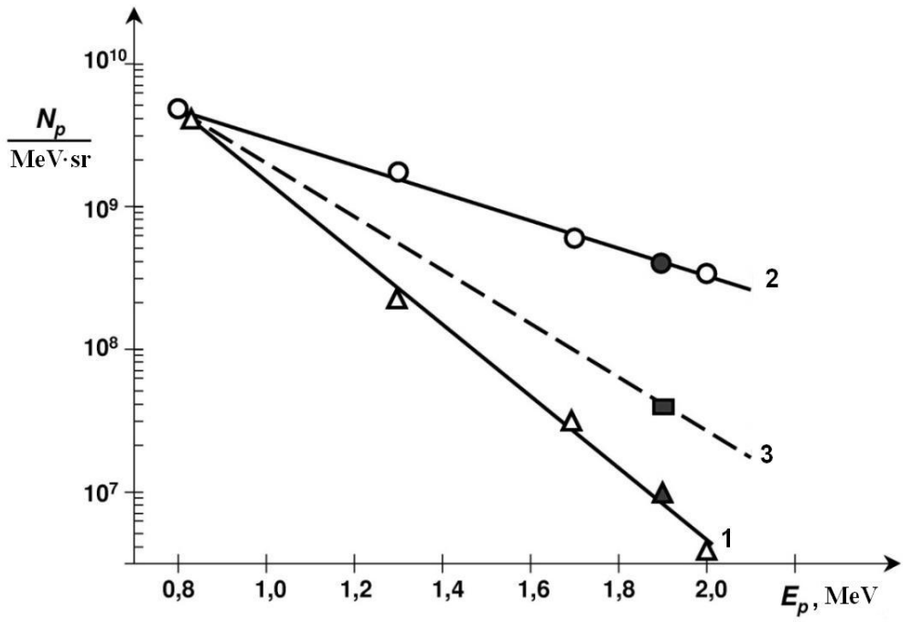


Fig. 5. Spectra of protons for various mechanisms of acceleration: (1) acceleration of protons from the front surface of the target toward a laser ray (Ti, 30 μm; $T \approx 180$ keV); (2) acceleration of protons from the rear surface of the target in the outward direction (Ti, 30 μm; $T \approx 500$ keV), and (3) acceleration of protons from the front surface of the target in the inward direction (LiF, 6 μm; $T \approx 250$ keV). The open circles and triangles represent data from track detectors, while the closed circles, triangles, and boxes stand for data obtained on the basis of the activation procedure [$p(^7\text{Li}, ^7\text{Be})n$, $E_{thr} = 1.88$ MeV].

Figure 6 shows the results of our experiments aimed at determining the maximum energy of protons for aluminum targets of various thickness—from 2.5 to 100 μm. These results were obtained both by using the CR-39 track detectors equipped with aluminum filters of various thickness and by using the activation procedure. From Fig. 6, one can see that there is an optimum aluminum-target thickness of 10 μm, at which protons of maximum energy 5 MeV are produced.

We will now compare the experimentally measured maximum energies of protons accelerated from the front surface of the target in the inward direction ($E \approx 2$ MeV) and protons accelerated from the rear surface of the target in the outward direction ($E \approx 5$ MeV) with the estimates of the maximum energy of protons subjected to the effect of the ponderomotive force (Pukhov, 2001),

$$E_{iMAX} \approx 2\sqrt{2} \cdot aZmc^2, \tag{22}$$

and in the case of plasma expansion into a vacuum (Zepf et al., 2003; Cowan et al., 2004; Robson et al., 2007),

$$E_{iMAX} \approx 2ZT_e \ln^2\left(\omega_{pi}\tau\right). \tag{23}$$

At $I = 2\times10^{18}$ W/cm², expression (22) yields the energy value of 1.73 MeV, while expression (23) leads to 5.1 MeV. These energy values agree reasonably well with experimental data.
We will now discuss the results obtained experimentally for the target-thickness dependence of the maximum energy of protons accelerated from the rare surface of the target in the outward direction. From our analysis, it follows that the reduction of the maximum proton energy at the foil thickness smaller than 10 μm is due to the effect of the nanosecond prepulse because of the pulse of enhanced spontaneous emission. The nanosecond prepulse generates shock waves in the foil, which deform the rear surface of the target, and this leads to a increase in the size of the plasma inhomogeneity at the rear surface of the target and to a decrease in the energy of protons produced at the rare surface of the target. The decrease in the maximum proton energy for target thicknesses in excess of 10 μm is due to the decrease in the energy of electrons as they pass through the target and to the increase of their angular spread. This in turn leads to a less efficient acceleration of protons from the rear surface of the target.

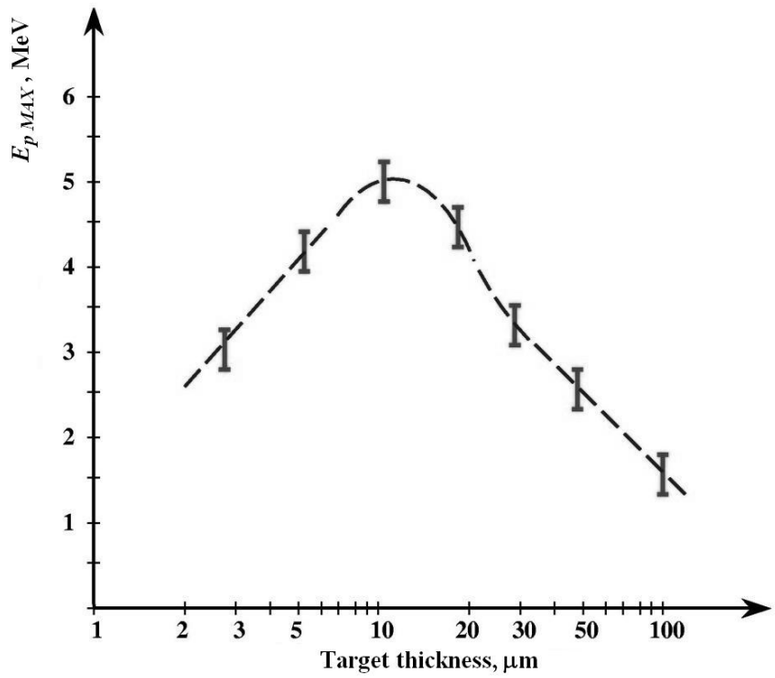


Fig. 6. Maximum proton energy $E_{pMAX}$ as a function of the aluminum-foil thickness.

In our paper (Belyaev et al., 2005), experimental data are presented on the generation of fast ions in a laser picosecond plasma at a laser radiation intensity of $2\times10^{18}$ W/cm². The results were obtained from Doppler spectra of hydrogen-like fluoride ions. An important peculiarity of the energy distribution of fast fluoride ions is the slow fall in ion energy to 1.4 MeV. In Fig. 7, the energy distribution of fast fluoride ions is plotted based on the results of measurements of $L_{ya}$ line profile for F IX ion. The solid curves are calculated by the formula

$$\frac{\mathrm{d}N}{\mathrm{d}E} \sim \exp\left[-\frac{M(v-v_0)^2}{2T_{fast}}\right] \tag{24}$$

where $v$ is the ion velocity in the observation direction, $Mv^2_0$ /2 = 25 keV, and the temperature of the fast fluoride ions is $T_{fast}$ = 350 keV.
In addition, using the red shift of the Doppler profile for the $L_{ya}$ line it was found that fast ions move inwards from a target surface. In (Belyaev et al., 2005), the parameters of the fluoride ion energy distribution were also estimated theoretically.

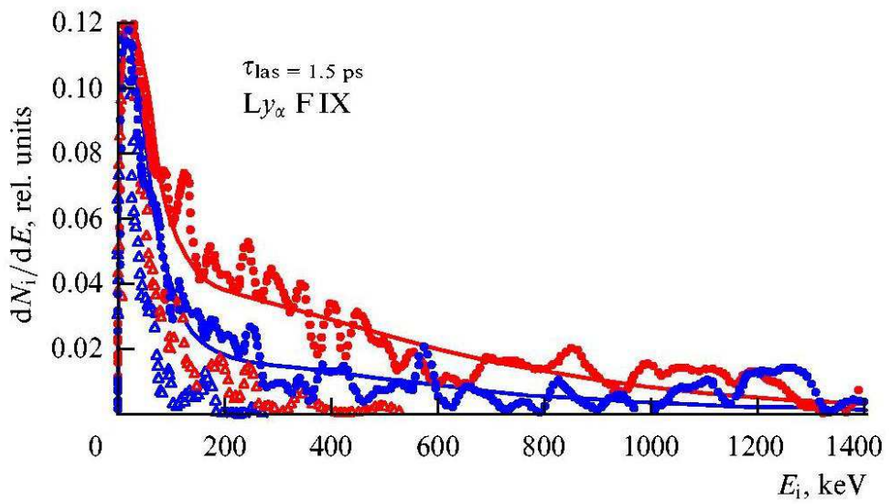


Fig. 7. Energy distribution of fast fluoride ions derived from the profile measurements of Lya line emitted by F IX ion. Top curve corresponds to ions moving towards the target, while bottom curve refers to ions moving outward from the target.

In our paper (Belyaev et al., 2009) the results of experiments devoted to studying the excitation of the promising nuclear fusion reactions $^6$Li($d$, $\alpha$)$^4$He, $^3$He($d$, $p$)$^4$He, $^{11}$B($p$, 3$\alpha$), and $^7$Li($p$, $\alpha$)$^4$He, along with the standard reaction D($d$, $n$)$^3$He, in picosecond laser plasmas are presented. For the first time, it was shown that these reactions may proceed at a moderate laser-radiation intensity of $2\times10^{18}$ W/cm$^2$, the respective yield being $2\times10^3$ to $10^5$ per laser pulse. A brief survey of the main processes responsible for the generation of fast electrons and fast ions (protons) at the front surface of the target and for the excitation of nuclear fusion reactions is given. The calculated and experimental results on the yield from nuclear fusion reactions in picosecond laser plasmas are compared. The possibilities for optimizing the yield from the promising fusion reactions excited in femto- and picosecond laser plasmas are discussed.

## 4. Relativistic magneto-active laser plasmas

Principal results of investigations of relativistic laser plasmas are presented here. We found parameters of magnetic fields generated in laser plasma – the amplitude of the magnetic field, its lifetime, and the increment, the spatial structure. Mechanisms of acceleration of charged particles have been investigated which are related with considered magnetic fields.
Main peculiarities that determine properties of relativistic laser plasmas are:

1. Electrons interacting with a field of electromagnetic wave can be considered as free particles.
2. Free electrons in relativistic laser plasmas interact only with an electromagnetic wave.

3. The conservation laws and motion integrals are valid also in the range of relativistic laser intensities.

Equations describing quasi-stationary magnetic fields which are generated in laser plasmas can be derived from the conservation law for generalized momentum:

$$\mathbf{P} = m\mathbf{v}\gamma - \frac{e}{c}\mathbf{A} \tag{25}$$

Here $\mathbf{A}$ is the vector-potential of an electromagnetic wave. The relativistic equation of motion is of the form

$$\frac{d}{dt} m\mathbf{v}\gamma = e\mathbf{E} + \frac{e}{c}\left[\mathbf{V} \times \mathbf{B}\right] \tag{26}$$

Deleting the intermediate derivations, we present final equations for vortex electron structures producing magnetic field in laser plasmas:

$$\boldsymbol{\omega} = rot\mathbf{v} \tag{27}$$

$$div\mathbf{V} = 0 \tag{28}$$

$$\frac{d\boldsymbol{\omega}}{dt} + rot\left[\boldsymbol{\omega} \times \mathbf{V}\right] = 0 \tag{29}$$

Here $\boldsymbol{\omega} = \frac{e\mathbf{B}}{mc\gamma}$ is a cyclotron frequency for electron rotation in the magnetic field $\mathbf{B}$, and $\gamma = 1\Big/\sqrt{1 - v^2/c^2}$ is the relativistic factor.

These equations mean conservation laws for vortex electron structure: Eq. (27) is the conservation law for a generalized momentum (25); Eq. (28) is the conservation law for a number of particles, and Eq. (29) is the conservation law for a magnetic flow, or for an angular momentum.

It should be noted that these equations allow undamped solutions. In general case solution of these equations taking into account losses is a difficult mathematical problem knowing as a problem of magnetic field generation. In particular, explanation of Earth magnetism is a part of this problem.

Equations (27) – (29) coincide with equations for real potential vortexes in mechanics of continuum matter which correspond to three Helmholtz theorems (Sedov, 1983).

The potential vortex presents good description of the observed vortex. Uniform rotation is unfit for description of the observed vortex. The velocity inside the observed vortex is high and outside of it is small, while the inverse statement is valid for the case of the uniform rotation. Coincidence of equations for a magnetic field in laser plasmas and for a potential vortex results in identity of their spatial structures (see Fig. 8).

An electron vortex producing a quasi-stationary magnetic field and their analogous classical potential vortex can exist only in motion. In general case the transformation of rotational energy into a translational motion is a relativistic effect. This fact follows from requirement of relativistic invariance for motion of charged particles; it takes place also at small non-

relativistic velocities. The expression for the motion integral follows from the equation (26), taking into account also the Maxwell equations for an electron in the field of an electromagnetic wave which propagates along the direction **n**:

$$\frac{1-\mathbf{n}\cdot\mathbf{v}/c}{\sqrt{1-V^2/c^2}} = Const \tag{30}$$

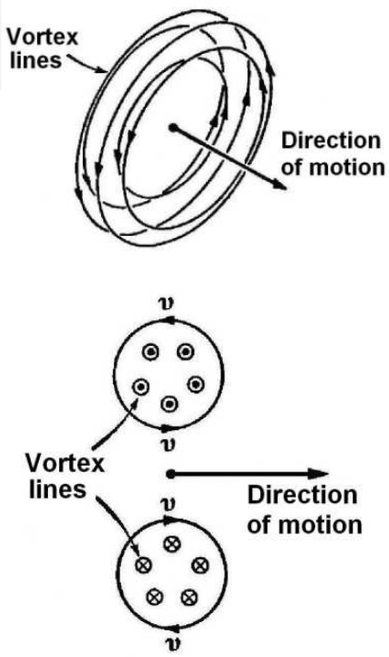


Fig. 8a. Vortex lines of moving potential vortex and its cross section

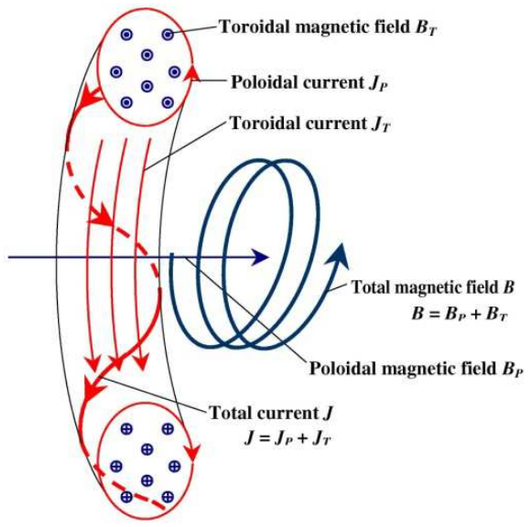


Fig. 8b. Structure of magnetic field produced in laser plasmas

This expression is useful at the consideration of dynamics of relativistic particles in a field of an electromagnetic wave. For example, if a charged particle (for example, an electron) rotates with the velocity $V$ in a circularly polarized field of an electromagnetic wave, then this particle acquires obligatory some velocity along the direction $\boldsymbol{n}$ of the wave propagation. When $\mathbf{V}/c = 0$, the expression (30) is equal to unity. This value does not change also for other velocities. Hence, one obtains the next expression for the particle velocity along the direction of propagation of electromagnetic wave:

$$\frac{V}{c} = \frac{\gamma - 1}{\gamma} = \frac{\sqrt{1+a^2}-1}{\sqrt{1+a^2}} \tag{31}$$

Here the quantity $a$ is determined by the electromagnetic wave intensity $J$: $a = 0{,}85\sqrt{\frac{J}{10^{18}}}$, $J$ [W/cm²].

Positively charged atomic ions prevent from motion of the considered electron vortex in a target because of the forces of the Coulomb attraction.

The requirement of quasi-neutrality results in motion of positively charged atomic ions. Omitting details of derivations and taking into account the Vlasov equations for a quasi-neutral two-component plasma and conservation law of the generalized momentum both for ions and for electrons, we present the final result:
Electrons and ions in relativistic laser plasmas form the one vortex structure – a potential vortex. This structure moves together with produced electromagnetic fields having the velocity of an electric drift (at **E** < **B**):

$$\mathbf{v} = c\frac{[\mathbf{EB}]}{\mathbf{B}^2} \tag{32}$$

Let us remark one peculiarity. The ion velocity and the ion free path are small in the process of ion motion. Ions are decelerated in a target; then new ions take their place, and finally the whole vortex structure occurs on the rear side of the target. If $l_i$ is the depth for ion deceleration, the last ions propagate together with electrons producing quasi-neutral potential plasma vortex.
The drift motion does not produce the electric current and charge separation, since particles with positive and negative charge drift in the same direction with the same velocity. Thus, drift produces motion of neutral plasma.
Plasma magnetization results in small divergence of these flows. It is explained by a stability of vortex quasi-neutral structures as quasi-particles
Some publications report about experimental confirmation of generation of magnetized toroidal plasma structures. Ring-shaped proton flows with small divergence were observed (Nakamura & Mima, 2008; Clark et al., 2000). The magnetic field of about 100 MG has been measured by direct spectral method on large distance (several hundreds of microns) from the target surface (Belyaev et al., 2004).
Our experiments at the peak laser intensity of $2\times10^{18}$ W/cm$^2$ allows us to observe on the rear side of thin (30 μm) titanium target clear ring-shaped structures by the proton detector CR-39 placed on a distance of 20 mm. Photo of ring-shaped proton structure is presented in Fig. 9a, and proton distributions with the energy of 2.5 MeV are presented in Fig. 9b. The divergence of the proton beam is $\varphi_{1/2} \approx 14°$. Protons with the energy higher than 2.5 MeV present narrow collimated beam with the divergence angle of $\varphi_{1/2} = 3°$. Inside this narrow collimated beam with the divergence angle $\varphi_{1/2} = 3°$ we observed well collimated proton beams with the divergence angle of $\varphi_{1/2} = 0.1°\div0.3°$.
Note, that drift velocity can increase significantly under condition of development of pinch-effect up to relativistic values. Respectively, not only electron velocity, but also the velocity of heavy positively charged atomic ions can increase up to relativistic values (Belyaev, Faenov et al., 2006).
Deleting the intermediate derivations, we present expressions for lifetime considered magnetic field:

$$T = 2\frac{\varepsilon}{\Delta\varepsilon}\Delta t \tag{33}$$

where $\varepsilon$ - laser pulse energy, $\Delta\varepsilon$ - losses of an energy for electron vortex structure, $\Delta t = \lambda^2/D$, $D$ – coefficient of Bohm's diffusion. This lifetime does not depend on duration of

laser action and can exceed it on one-two order. For this reason the superstrong magnetic fields generated in laser plasma, term quasistationary.
Increment of the considered magnetic field is equal to the ionization rate $\omega_i$, which is larger than the plasma frequency.

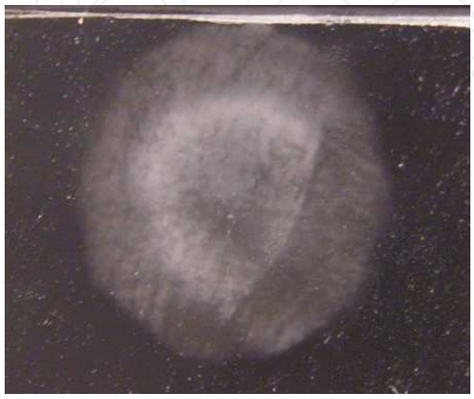

Fig. 9a. The photo of the track detector CR-39 covered by 11 mm Al filter. Detector CR-39 shows the tracks of protons with energies $E_p$ > 0.8 MeV; $\varphi_{1/2}$ » 14° (cone half angle)

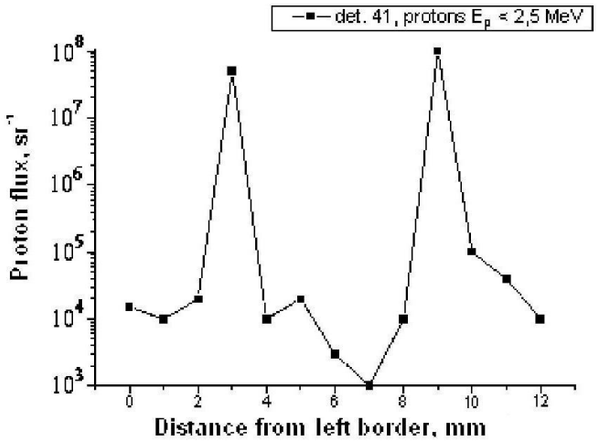


Fig. 9b. The proton distribution inside the spot for detector with 11 μm Al ($E_p$ > 0.8 MeV). Target Cu 25 μm. Protons with energy $E$ < 2,5 MeV

Mechanisms of generating magnetic fields are a subject of numerous investigations performed in recent years (Tatarakis et al., 2002; Beg et al., 2004; Borghesi et al., 1998). Various mechanisms for generating a magnetic field in the interaction of intensive laser radiation with solid targets are described in a number of theoretical works (Stamper, 1991; Wilks et al., 1992; Bell et al., 1993; Buchenkov et al., 1993; Sudan, 1993; Haines, 1997; Mason & Tabak, 1998; Krainov, 2003). In particular, they predicted the origin of magnetic fields with induction of up to 1GG in the dense plasma produced during the interaction process. These fields are localized near the critical surface, where the laser energy is mainly absorbed. The arising magnetic fields noticeably affect the dynamics of laser plasma. The principal mechanisms of generating quasistatic magnetic fields were considered: (1) different directions of the temperature and plasma density gradients; (2) the flux of fast electrons accelerated by ponderomotive forces in the longitudinal and transversal directions with respect to the direction of laser pulse propagation, and (3) the collisionless Weibel instability (Weibel, 1959).
Measurements of superstrong quasistatic magnetic fields in laser plasma and their theoretical interpretation have been discussed in more detail in our article (Belyaev et al., 2008).
Measurements of magnetic fields in plasma by various independent methods are very important for both proving the existence of such fields and determining their spatial structure (topology). For this purpose, we measured the profiles of X-ray spectral lines of hydrogen-like fluoride ions in laser plasma with a radiation intensity of $10^{17}$ W/cm$^2$ and

pulse duration of 1 ps (Belyaev et al., 2004). The structure observed is characterized by distinct dips and peaks on the spectral line profiles (see Fig. 10). These features can be explained by invoking a conception of the strong turbulent noise that develops in the superstrong magnetic field generated in laser plasma.

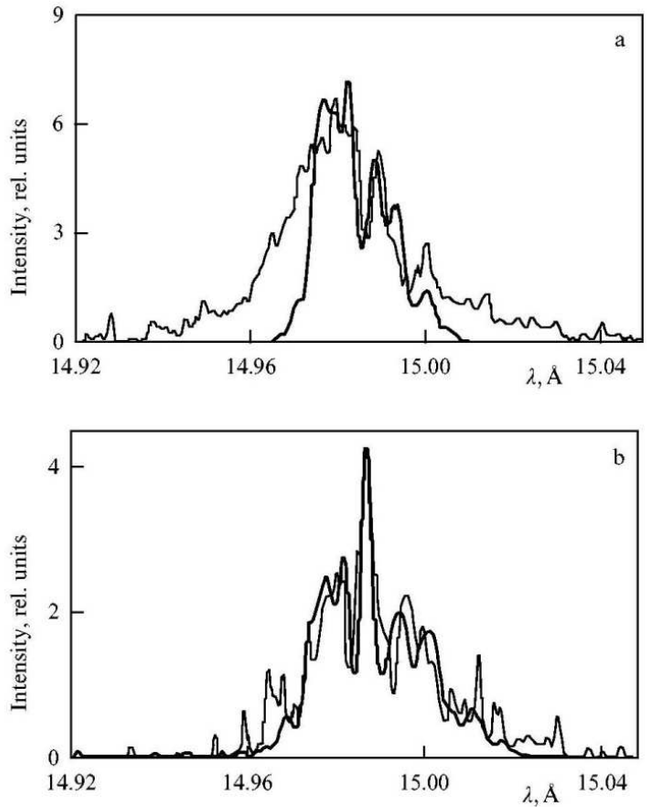


Fig. 10. Comparison of experimental (thin curves) and theoretical (thick curves) profiles for the $L_{\gamma a}$ line of F IX ion: (a) the experiment was performed at $I_{las} = 2\times10^{17}$ W/cm$^2$, and calculation was made at $T_i = 100$ eV, $n_e = 10^{20}$ cm$^{-3}$, $\omega = 7\times10^{14}$ s$^{-1}$, $E_0 = 4\times10^8$ V/cm; (b) the experimental $I_{las} = 3\times10^{17}$ W/cm$^2$, and the calculation was done at $T_i = 100$ eV, $n_e = 2\times10^{20}$ cm$^{-3}$, $\omega = 10^{15}$ s$^{-1}$, and $E_0 = 6\times10^8$ V/cm.

## 5. Conclusion

The above-described mechanisms for accelerating electrons and ions to a greater or lesser degree comply with up-to-date concepts on the generation of fast particles in laser plasma. According to these concepts, the energy of an initial laser pulse is converted to the energy of electron motion. The mechanisms for such energy conversion are mainly related to (1) a ponderomotive potential; (2) a phase interruption of electron oscillations in the laser wave due to various mechanisms, among which the main one is electron ejection beyond the sharp boundary of a target (vacuum heating), and (3) various resonance mechanisms where the electron motion is at resonance with plasma waves (wake-field resonance absorption or acceleration) or the cyclotron or betatron oscillation of an electron in the channel produced by laser radiation in the presence of a magnetic field. Ion acceleration in this case is a

secondary effect mainly caused by the electric fields of the spatial charge produced when fast accelerated electrons are separated from ions. The detailed distribution of such fields substantially depends on the target thickness, which makes a difference in the ion acceleration at the front and rear target surfaces.

As a whole, particle acceleration is characterized by the multifactor character of the parameters involved. Such parameters are the intensity, frequency, and duration of the laser pulse; the contrast, which determines pre-plasma parameters; the thickness and structure of the target; the presence of magnetic fields, and some other factors. By combining these parameters, one can reach the optimal (in certain limits) conditions of particle acceleration. There is a wide range of various applications of such laser-driven accelerators, starting from fundamental investigations concerning nuclear processes for isotope production, to the initiation of thermonuclear reactions using laser setups that are quite small in size compared to standard accelerators, and ending by particular applications such as sources of proton radiation for medical purposes.

Nevertheless, there are a sufficiently large number of problems to be solved related to particle acceleration. These are, for example, ion beam focusing and annular structures arising in the beam. In electron acceleration, the problem of forming a monoenergetic beam of fast electrons with a maximum energy has not yet been solved.

As far as the generation of super-strong magnetic fields is concerned, the main problems are determination of their lifetime and topology. Experimental results definitely indicate that the lifetimes of magnetic fields are considerably longer (by orders of magnitude) than the laser pulse duration.

From our point of view, this is direct evidence that long-living magnetic configurations exist in laser plasma. This is also confirmed by investigations into the dynamics of pinch structures in irradiating wire targets by laser pulses. The topology and dynamics of such structures are, as was noted above, in surprisingly good agreement with those obtained under the pulse action of mega-ampere currents.

It is clear that the presence of high-intensity fast particles and magnetic fields in plasma, in addition to the specific features of particle acceleration mentioned above, should result in numerous instabilities arising in plasma. This is directly illustrated by the results mentioned above on measuring the profiles of spectral lines for multiply charged ions. Profile irregularity is indicative of the existence of intense electrostatic oscillations possessing definite frequencies and intensities. Thus, in view of all the specific features mentioned above, one can conclude that in the case of ultra-short laser pulses we are dealing with magneto-active turbulent plasma, numerous properties of which are not clear presently. Nevertheless, it is possible to choose sufficiently optimal conditions for generating high-energy charged particles in such plasmas.

## 6. Acknowledgment

This research has been supported by the Russian Foundation for Basic Research, projects NN 09-02-00041, 10-02-01095, 10-08-00752, 11-02-12026.

## 7. References

Andreev, A.V.; Gordienko, V.M. & Savel'ev, A.B. (2001). Nuclear processes in a high-temperature plasma produced by an ultrashort laser pulse. *Quantum Electronics*, Vol.31, No.11, (November 2001), pp. 941-956, ISSN 0018-9197

Amiranoff, F.; Baton, S.; Bernard, D.; Cros, B.; Descamps, D.; Dorchies, D.; Jacquet, F.; Malka, V.; Marques, J.R.; Matthieussent, G.; Mine, P.; Modena, A.; Mora, P.; Morillo, J. & Najmudin, Z. (1998). Observation of Laser Wakefield Acceleration of Electrons. *Physical Review Letters*, Vol.81, No.5, (August 1998), pp.995-998, ISSN 0031-3727

Beg, F.N.; Clark, E.L.; Wei, M.S.; Dangor, A.E.; Evans, R.G.; Gopal, A.; Lancaster, K.L.; Ledingham, K.W.D.; McKenna, P.; Norreys, P.A.; Tatarakis, M.; Zepf, M. & Krushelnick, K. (2004). High-Intensity-Laser-Driven *Z* Pinches. *Physical Review Letters*, Vol.92, No.9, (March 2004), pp. 095001, ISSN 0031-9007

Bell, A.R.; Beg, F.N.; Chang, Z.; Dangor, A.E.; Danson, C.N.; Edwards, C.B.; Fews, A.P.; Hutchinson, M.H.R.; Luan, S.; Lee, P.; Norreys, P.A.; Smith, R.A.; Taday, P.F. & Zhou, F. (1993). Observation of plasma confinement in picosecond laser-plasma interactions. *Physical Review E*, Vol.48, No.3, (September 1993), pp.2087-2093, ISSN 1539-3755

Belyaev, V.S. & Mikhailov, V.N. (2001). Quantum Plasmas: Criteria, Anomalous Diffusion, and Bleaching in a Magnetic Field. *Laser Physics*, Vol.11, No.8, (December 2000), pp.957-973, ISSN 1054-660X

Belyaev, V. S.; Kostenko, O.F. & Lisitsa, V.S. (2003). Cyclotron mechanism of electron acceleration in subpicosecond laser plasma. *Letters to Jounal of Experimental and Theoretical Physics*, Vol.77, No.12, (June 2003), pp.653-656, ISSN 0021-3640

Belyaev, V.S. (2004). Mechanism of high-energy electron production in a laser plasma. *Quantum Electronics*, Vol.34, No.1, (January 2004), pp.41-46, ISSN 0018-9197

Belyaev, V.S.; Vinogradov, V.I.; Kurilov, A.S.; Matafonov, A.P.; Lisitsa, V.S.; Gavrilenko, V.P.; Faenov, A.Ya.; Pikuz, T.A.; Skobelev, I.Yu.; Magunov, A.I. & Pikuz, S.A. Jr. (2004). Plasma Satellites of X-ray Lines of Ions in a Picosecond Laser Plasma. *Journal of Experimental and Theoretical Physics*, Vol.99, No.4, (April 2004), pp. 708-719, ISSN 1090-6509

Belyaev, V.S.; Vinogradov, V.I.; Matafonov, A.P.; Krainov, V.P.; Lisitsa, V.S.; Faenov, A.Ya.; Pikuz, T.A.; Skobelev, I.Yu.; Magunov, A.I.; Pikuz, S.A. Jr.; Andrianov, V.P.; Ignat'ev, G.N.; Kozhunov, Yu.I.; Kozlov, O.B. & Chekmarev, A.M. (2005). Effective Temperature and the Directional Motion of Fast Ions in a Picosecond Laser Plasma. *Letters to Jounal of Experimental and Theoretical Physics*, Vol.81, No.12, (May 2005), pp.616-620, ISSN 0021-3640

Belyaev, V.S.; Faenov, A.Ya.; Magunov, A.I.; Matafonov, A.P.; Pikuz, T.A.; Pikuz S.A.Jr., Skobelev, I.Yu. & Vinogradov, V.I. (2006). Directed inward beams of ions in laser produced plasma. *Journal De Physique IV France*, Vol.133, No., (June 2006), pp. 525-527, ISBN 2-86883-925-8

Belyaev, V.S.; Vinogradov, V.I.; Matafonov, A.P.; Krainov, V.P.; Lisitsa, V.S.; Andrianov, V.P. & Ignatyev, G.N. (2006). Effect of Prepulses with Various Durations on the Neutron Yield in Laser Picosecond Plasma. *Laser Physics*, Vol.16, No.12, (December 2006), pp.1647-1657, ISSN 1054-660X

Belyaev, V.S.; Krainov, V.P.; Lisitsa, V.S. & Matafonov, A.P. (2008). Generation of fast charged particles and superstrong magnetic fields in the interaction of ultrashort high-intensity laser pulses with solid targets. *Physics – Uspekhi*, Vol.51, No.8, (August 2008), pp. 793-814, ISSN 1063-7869

Belyaev, V.S.; Vinogradov, V.I.; Matafonov, A.P.; Rybakov, S.M.; Krainov, V.P.; Lisitsa, V.S.; Andrianov, V.P.; Ignatiev, G.N.; Bushuev, V.S.; Gromov, A.I.; Rusetsky, A.S. &

Dravin, V.A. (2009). Excitation of Promising Nuclear Fusion Reactions in Picosecond Laser Plasmas. *Physics of Atomic Nuclei*, Vol.72, No.7, (September 2009) pp.1077–1098, ISSN 1063-7788

Borghesi, M.; MacKinnon, A.J.; Bell, A.R.; Gaillard, R. & Willi, O. (1998). Megagauss Magnetic Field Generation and Plasma Jet Formation on Solid Targets Irradiated by an Ultraintense Picosecond Laser Pulse. *Physical Review Letters*, Vol.81, No.1, (July 1998), pp.112-115, ISSN 0031-3727

Borodin, V.G.; Gilev, O.N.; Zapysov, A.L.; Komarov, V.M.; Lykov, V.A.; Malinov, V.A.; Migel', V.M.; Nikitin, N.V.; Pokrovskii, V.G.; Pronin, V.A.; Saprykin, V.N.; Charukhchev, A.V. & and Chernov, V.N. (2000). Hard X Radiation and Fast Particles in Laser Plasma Experiments at Laser Intensities of up to $5\times10^{18}$ W/cm$^2$ on the Target Surface. *Letters to Jounal of Experimental and Theoretical Physics*, Vol.71, No.6, (April 1999), pp.246-250, ISSN 0021-3640

Brunel, F. (1987). Not-so-resonant, resonant absorption. *Physical Review Letters*, Vol.59, No.1, (July 1987), pp.52-55, ISSN 0031-3727

Bychenkov V.Yu., Kasyanov, Yu.S.; Sarkisov, G.S. & Tikhonchuk, V.T. (1993). Mechanism of generation of magnetic fields in laser plasma study. *Letters to Jounal of Experimental and Theoretical Physics*, Vol.58, No., (1993), pp.184-, ISSN 0021-3640

Carrier, M.; Lefebvre, E.; Flacco, A. & Malka, V. (2009). Influence of subpicosecond laser pulse duration on proton acceleration. *Physics of Plasmas*, Vol.16, No.5, (May 2009), pp.053105, ISSN 1070-664X

Clark, E.L.; Krushelnick, K.; Zepf, M.; Beg, F.N.; Tatarakis, M.; Machacek, A.; Santala, M.I.K.; Watts, I.; Norreys, P.A. & Dangor, A.E. (2000). Energetic Heavy-Ion and Proton Generation from Ultraintense Laser-Plasma Interactions with Solids. *Physical Review Letters*, Vol.85, No.8, (August 2000), pp.1654-1657, ISSN 0031-3727

Cowan, T.E.; M.D. Perry, M.D.; Key, M.H.; Ditmire, T.R.; Hatchett, S.P.; Henry, E.A.; Moody, J.D.; Moran, M.J.; Pennington, D.M.; Phillips, T.W.; Sangster, T.C.; Sefcik, J.A.; Singh, M.S.; Snavely, R.A.; Stoyer, M.A.; Wilks, S.C.; Young, P.E.; Takahashi, Y.; Dong, B.; Fountain, W.; T. Parnell, T.; Johnson, J.; Hunt, A.W. & and Kuhl, T. (1999). High energy electrons, nuclear phenomena and heating in petawatt laser-solid experiments. *Laser and Particle Beams*, Vol.17, No.4, (October 1999), pp.773-783, ISSN 0263-0346

Cowan, T.E.; Fuchs, J.; Ruhl, H.; Kemp, A.; Audebert, P.; Roth, M.; Stephens, R.; Barton, I.; Blazevic, A.; Brambrink, E.; Cobble, J.; Fernandez, J.; Gauthier, J.-C.; Geissel, M.; Hegelich, M.; Kaae, J.; Karsch, S.; Le Sage, G.P.; Letzring, S.; Manclossi, M.; Meyroneinc, S.; Newkirk, A.; Pepin, H. & Renard-LeGalloudec, N. (2004). Ultralow Emittance, Multi-MeV Proton Beams from a Laser Virtual-Cathode Plasma Accelerator. *Physical Review Letters*, Vol.92, No.20, (May 2004), pp.204801, ISSN 0031-3727

Demchenko, N.N. & Rozanov, V.B. (2001). A Hydrodynamic Model of the Interaction of Picosecond Laser Pulses with Condensed Targets. *Journal of Russian Laser Research*, Vol.22, No.3, (May 2001), pp.228-242, ISSN 1071-2836

Esarey, E.; Sprangle, P.; Krall, J. & Ting, A. (1996). Overview of plasma-based accelerator concepts. *IEEE Transaction on Plasma Science*, Vol.24, No.2, (April 1996), pp.252-288, ISSN 0093-3813

Fukuda, Y.; Faenov, A.Ya.; Tampo, M.; Pikuz, T.A.; Nakamura, T.; Kando, M.; Hayashi, Y.; Yogo, A.; Sakaki, H.; Kameshima, T.; Pirozhkov, A.S.; Ogura, K.; Mori, M.; Esirkepov, T.Zh.; Koga, J.; Boldarev, A.S.; Gasilov, V.A.; Magunov, A.I.; Yamauchi, T.; Kodama, R.; Bolton, P.R.; Kato, Y.; Tajima, T.; Daido, H. & Bulanov, S.V. (2009). Energy Increase in Multi-MeV Ion Acceleration in the Interaction of a Short Pulse Laser with a Cluster-Gas Target. *Physical Review Letters*, Vol.103, No.16, (October 2009), pp.165002, ISSN 0031-3727

Haines, M.G. (1997). Saturation Mechanisms for the Generated Magnetic Field in Nonuniform Laser-Matter Irradiation. *Physical Review Letters*, Vol.78, No.2, (January 1997), pp.254-257, ISSN 0031-3727

He, F.; Yu, W.; Lu, P.; Xu, H.; Qian, L.; Shen, B.; Yuan, X.; Li, R. & Xu, Z. (2004). Ponderomotive acceleration of electrons by a tightly focused intense laser beam. *Physical Review E*, Vol.68, No.4, (October 2004), pp.046407, ISSN 1539-3755

Huang, L.G.; Lei, A.L.; Bin J.N.; Bai, Y.; Wei Yu; Yu, M.Y. & Cowan, T.E. (2010). Improving proton acceleration with circularly polarized intense laser pulse by radial confinement with heavy ions. *Physics of Plasmas*, Vol.17, No.1, (January 2010), pp.013106, ISSN 1070-664X

Gonoskov, A.A.; Korzhimanov, A.V.; Eremin, V.I.; Kim, A.V. & Sergeev, A.M. (2009). Multicascade Proton Acceleration by a Superintense Laser Pulse in the Regime of Relativistically Induced Slab Transparency. *Physical Review Letters*, Vol.102, No.18, (May 2009), pp.184801, ISSN 0031-3727

Gus'kov, S.Yu.; Demchenko, N.N.; Makarov, K.N.; Nishchuk, S.G.; Pikuz, T.A.; Satov, Yu.A.; Skobelev, I.Yu.; Smakovski, Yu.B.; Faenov, A.Ya.; Khomenko, S.V. & Sharkov, B.Yu. (2001). Influence of Angles of Incidence of Laser Radiation on the Generation of Fast Ions. *Letters to Jounal of Experimental and Theoretical Physics,* Vol.73, No.12, (May 2001), pp.665-661, ISSN 0021-3640

Krainov, V. P. (2003). Generation of high magnetic fields in an atomic plasma by irradiation with a super-intense femtosecond laser pulse. *Journal of Physics B: Atomic, Molecular and Optical Physics*, Vol.36, No.15, (August 2003), pp.3187-3202, ISSN 0953-4075

Ledingham, K.W.D. & Norreys, P.A. (1999). Nuclear physics merely using a light source. *Contemporary Physics*, Vol.40, No.6, (December 1999), pp.367-383, ISSN 0010-7514

Mackinnon, A.J.; Borghesi, M.; Hatchett, S.; Key, M.H.; Patel, P.K.; Campbell, H.; Schiavi, A.; Snavely, R.; Wilks, S.C. & Willi, O. (2001). Effect of Plasma Scale Length on Multi-MeV Proton Production by Intense Laser Pulses. *Physical Review Letters*, Vol.86, No.9, (February 2001), pp.1769-1772, ISSN 0031-3727

Maksimchuk, A.; Gu, S.; Flippo, K.; Umstadter, D. & Bychenkov, V.Yu. (2000). Forward Ion Acceleration in Thin Films Driven by a High-Intensity Laser. *Physical Review Letters*, Vol.84, No.18, (May 2000), pp.4108-4111, ISSN 0031-3727

Malka, G. & Miquel, J.L. (1996). Experimental Confirmation of Ponderomotive-Force Electrons Produced by an Ultrarelativistic Laser Pulse on a Solid Target. *Physical Review Letters*, Vol.77, No.1, (July 1996), pp.75-78, ISSN 0031-3727

Mangles, S.P.D.; Walton, B.R.; Tzoufras, M.; Najmudin, Z.; Clarke, R.J.; Dangor, A.E.; Evans, R.G.; Fritzler, S.; Gopal, A.; Hernandez-Gomez, C.; Mori, W.B.; Rozmus, W.; Tatarakis, M.; Thomas, A.G.R.; Tsung, F.S.; Wei, M.S. & Krushelnick, K. (2005). Electron Acceleration in Cavitated Channels Formed by a Petawatt Laser in Low-

Density Plasma. *Physical Review Letters*, Vol.94, No.24, (June 2005), pp.245001, ISSN 0031-3727

Mason, R. J. & Tabak, M. (1998). Magnetic Field Generation in High-Intensity-Laser–Matter Interactions. *Physical Review Letters*, Vol.80, No.3, (January 1998), pp.524-527, ISSN 0031-3727

Matafonov, A. & Belyaev, V. (2001). Experimental Investigation of Gamma and Neutron Radiation from Laser Produced Plasma, *Proceedings of 28th EPS Conference on Controlled Fusion and Plasma Physics-2001*, Funchal, Madeira, Portugal, 18 - 22 June, 2001, http://www.cfn.ist.utl.pt/EPS2001/

Mourow, G.A.; Tajima, T. & Bulanov, S.V. (2006). Optics in the relativistic regime. *Review of Modern Physics*, Vol.78, No.2, (April 2006), pp. 309-371, ISSN 0034-6861

Nakamura, T. & Mima, K. (2008) . Magnetic-Dipole Vortex Generation by Propagation of Ultraintense and Ultrashort Laser Pulses in Moderate-Density Plasmas. *Physical Review Letters*, Vol.100, No.20, (May 2008), pp.205006, ISSN 0031-3727

Nickles, P.V.; Kalachnikov, M.P.; Warwick, P.J.; Janulewicz, K.A.; Sandner, W.; Jahnke, U.; Hilscher, D.; Schnurer, M.; Nolte, R. & Rousse, A. (1999). Energetic electrons and x-ray photons from multiterawatt Ti:sapphire lasers. *Quantum Electronics*, Vol.29, No.5, (May 1999), pp.444-448, ISSN 0018-9197

Pavlenko, Yu.G. (2002). *Lectures on theoretical mechanics*, FIZMATLIT, ISBN 5-9221-0241-9, Moscow (in russian)

Pukhov, A. (2001). Three-Dimensional Simulations of Ion Acceleration from a Foil Irradiated by a Short-Pulse Laser. *Physical Review Letters*, Vol.86, No.16, (April 2001), pp.3562-3565, ISSN 0031-3727

Psikal, J.; Tikhonchuk, V.T.; Limpouch, J. & Klimo, O. Lateral. (2010). Lateral hot electron transport and ion acceleration in femtosecond laser pulse interaction with thin foils. *Physics of Plasmas*, Vol.17, No.1, (January 2010), pp.013102, ISSN 1070-664X

Pukhov, A.; Sheng, Z-M. & Meyer-ter-Vehn, J. (1999). Particle acceleration in relativistic laser channels. *Physics of Plasmas*, Vol.6, No.7, (April 1999), pp.2847-2855, ISSN 1070-664X

Robson, L.; Simpson, P.T.; Clarke, R.J.; Ledingham, K.W.D.; Lindau, F.; Lundh, O.; McCanny, T.; Mora, P.; Neely, D.; Wahlstrom, C.-G.; Zepf, M. & McKenna, P. (2007). Scaling of proton acceleration driven by petawatt-laser–plasma interactions. *Nature Physics*, Vol.3, No., (December 2007), pp.58-62, ISSN 1745-2473

Salamin, Y.I.; Hu, S.X.; Hatsagortsyan, K.Z. & Keitel, C.H. (2006). Relativistic high-power laser–matter interactions. *Physical Reports*, Vol.427, No.2-3, (April 2006), pp.41-155, ISSN 0370-1573

Sedov, L.I. (1983). *Mechanics of continuum matter* (Vol. 1), ISBN 978-3-540-88467-5, Nauka, Moscow

Sentoku, T.; Cowan, T.E.; Kemp, A. & Ruhl, H. (2003). High energy proton acceleration in interaction of short laser pulse with dense plasma target. *Physics of Plasmas*, Vol.10, No.5, (December 2003), pp.2009-2016, ISSN 1070-664X

Stamper, J.A. (1991). Review on spontaneous magnetic fields in laser-produced plasmas: Phenomena and measurements. *Laser and Particle Beams*, Vol.9, No.4, (March 1991), pp.841-862, ISSN 0263-0346

Sudan, R.N. (1993). Mechanism for the generation of $10^9$ G magnetic fields in the interaction of ultraintense short laser pulse with an overdense plasma target. *Physical Review Letters*, Vol.70, No.20, (May 1993), pp.3075-3078, ISSN 0031-3727

Tatarakis, M. ; Gopal, A.; Watts, I.; Beg F.N.; Dangor, A.E.; Krushelnick, K.; Wagner, U.; Norreys, P.A.; Clark, E.L.; Zepf, M. & Evans, R.G. (2002). Measurements of ultrastrong magnetic fields during relativistic laser–plasma interactions. *Physics of Plasmas*, Vol.9, No.5, (May 2002), pp. 2244-2250, ISSN 1070-664X

Umstadter, D. (2003). Relativistic laser–plasma interactions. *Journal of Physics D: Applied Physics*, Vol.36, No.8, (April 2003 ), pp. R151-R165, ISSN 0022-3727

Weibel, E.S. (1959). Spontaneously Growing Transverse Waves in a Plasma Due to an Anisotropic Velocity Distribution. *Physical Review Letters*, Vol.2, No.3, (February 1959), pp.83-84, ISSN 0031-3727

Wilks, S.C.; Kruer, W.L.; Tabak, M. & Langdon, A.B. (1992). Absorption of Ultra-Intense Laser Pulses. *Physical Review Letters*, Vol.69, No.9, (August 1992), pp.1383-1386, ISSN 0031-3727

Wilks, S.C.; Langdon, A.B.; Cowan, T.E.; Roth, M.; Singh, M.; Hatchett, S.; Key, M.H.; Pennington, D.; MacKinnon, A. & Snavely, R.A. (2001). Energetic proton generation in ultra-intense laser–solid interactions. *Physics of Plasmas*, Vol.8, No.2, (August 2001), pp.542-550, ISSN 1070-664X

Willingale, L.; Nagel, S.R.; Thomas, A.G.R.; Bellei, C.; Clarke, R.J.; Dangor, A.E.; Heathcote, R.; Kaluza, M.C.; Kamperidis, C.; Kneip, S.; Krushelnick, K.; Lopes, N.; Mangles, S.P.D.; Nazarov, W.; Nilson, P.M. & Najmudin, Z. (2009). Characterization of High-Intensity Laser Propagation in the Relativistic Transparent Regime through Measurements of Energetic Proton Beams. *Physical Review Letters*, Vol.102, No.12, (March 2009), pp.125002, ISSN 0031-3727

Yan, X.Q.; Wu, H.C.; Sheng, Z.M.; Chen, J.E. & Meyer-ter-Vehn, J. (2009). Self-Organizing GeV, Nanocoulomb, Collimated Proton Beam from Laser Foil Interaction at $7\times10^{21}$ W/cm$^2$. *Physical Review Letters*, Vol.103, No.13, (September 2009), pp.135001 (2009), ISSN 0031-3727

Youssef, A.; R. Kodama, R. & M. Tampo, M. (2006). Study of proton acceleration at the target front surface in laser-solid interactions by neutron spectroscopy. *Physics of Plasmas*, Vol.13, No.3, (March 2006), pp.030702, ISSN 1070-664X

Zepf, M.; Clark, E.L.; Beg, F.N.; Clarke, R.J.; Dangor, A.E.; Gopal, A.; Krushelnick, K.; Norreys, P.A.; Tatarakis, M.; Wagner, U. & and Wei, M.S. (2003). Proton Acceleration from High-Intensity Laser Interactions with Thin Foil Targets. *Physical Review Letters*, Vol.90, No.6, (February 2003), pp.064801, ISSN 0031-3727

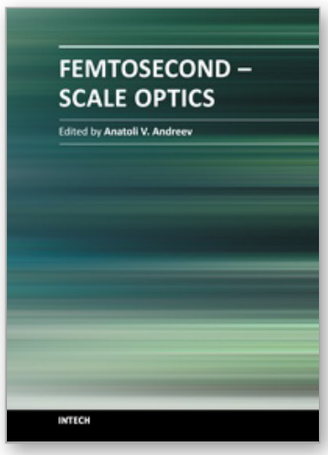


**Femtosecond-Scale Optics**
Edited by Prof. Anatoly Andreev

ISBN 978-953-307-769-7
Hard cover, 434 pages
**Publisher** InTech
**Published online** 14, November, 2011
**Published in print edition** November, 2011

With progress in ultrashort ultraintense laser technologies the peak power of a laser pulse increases year by year. These new instruments accessible to a large community of researchers revolutionized experiments in nonlinear optics because when laser pulse intensity exceeds or even approaches intra-atomic field strength the new physical picture of light-matter interaction appears. Laser radiation is efficiently transformed into fluxes of charged or neutral particles and the very wide band of electromagnetic emission (from THz up to x-rays) is observed. The traditional phenomena of nonlinear optics as harmonic generation, self-focusing, ionization, etc, demonstrate the drastically different dependency on the laser pulse intensity in contrast the well known rules. This field of researches is in rapid progress now. The presented papers provide a description of recent developments and original results obtained by authors in some specific areas of this very wide scientific field. We hope that the Volume will be of interest for those specialized in the subject of laser-matter interactions.

**How to reference**
In order to correctly reference this scholarly work, feel free to copy and paste the following:

Vadim Belyaev and Anatoly Matafonov (2011). Fast Charged Particles and Super-Strong Magnetic Fields Generated by Intense Laser Target Interaction, Femtosecond-Scale Optics, Prof. Anatoly Andreev (Ed.), ISBN: 978-953-307-769-7, InTech, Available from: http://www.intechopen.com/books/femtosecond-scale-optics/fast-charged-particles-and-super-strong-magnetic-fields-generated-by-intense-laser-target-interactio

INTECH
open science | open minds

**InTech Europe**
University Campus STeP Ri
Slavka Krautzeka 83/A
51000 Rijeka, Croatia
Phone: +385 (51) 770 447
Fax: +385 (51) 686 166
www.intechopen.com

**InTech China**
Unit 405, Office Block, Hotel Equatorial Shanghai
No.65, Yan An Road (West), Shanghai, 200040, China
中国上海市延安西路65号上海国际贵都大饭店办公楼405单元
Phone: +86-21-62489820
Fax: +86-21-62489821

© 2011 The Author(s). Licensee IntechOpen. This is an open access article distributed under the terms of the Creative Commons Attribution 3.0 License, which permits unrestricted use, distribution, and reproduction in any medium, provided the original work is properly cited.

IntechOpen

IntechOpen